Quaternary International 443 (2017) 39–48

Contents lists available at ScienceDirect

Quaternary International

journal homepage: www.elsevier.com/locate/quaint

Palaeoclimatic reconstruction by using the varvite sediments of Bharatpur, Upper Lahaul Valley, NW Himalaya, India

Archna Bohra [a,*], Bahadur Singh Kotlia [b], Nathani Basavaiah [c]

[a] Centre for Glaciology, Wadia Institute of Himalayan Geology, Dehradun, India
[b] Centre for Advanced Study in Geology, Kumaun University, Nainital, India
[c] Indian Institute of Geomagnetism, New Panvel, Navi Mumbai, India

ARTICLE INFO

Article history:
Received 9 November 2016
Received in revised form
10 April 2017
Accepted 25 April 2017
Available online 3 May 2017

Keywords:
Varvite sediments
Lahaul Himalaya
Mineral magnetism
Geochemical data
Palaeoclimatic changes
Quaternary period

ABSTRACT

A 6 m thick varvite profile exposed at Bharatpur (77° 27′ E: 32° 48′ N, altitude 4692 m) in the NW Himalaya was investigated to understand the past climatic signatures during the Late Quaternary period. The radiocarbon chronology brackets the varvite sedimentation between ~24.3 and 7.2 ka BP and the sedimentary sequence is bounded by river born gravel at the top and glacial outwash at the bottom. The proxies used were lithology, chronology (AMS/radiocarbon dating), geochemical analysis, loss on ignition (LOI), and mineral magnetism. Other parameters, e.g., Chemical Index of Alteration (CIA), Chemical Index of Weathering (CIW), Al_2O_3/SiO_2, Fe_2O_3, CaO, MgO and Al/Na ratio were also used. Based on the combined data set, six phases of warm and cold climatic conditions are reconstructed. The mean CIA, CIW and Al/Na ratios reveal that the sediments were incorporated from sedimentary rocks by moderate silicate chemical weathering process. Based on the available chronology, the basal most glacial outwash event can be estimated as ca. 24.3 ka BP and the laminated section shows continuity of sedimentation from the Late Quaternary to Holocene. The period between ~ ca. 24.3 and 22.6 ka can be regarded as an arid phase. From ~ ca. 22.6–20.5 ka BP, a slight increase in monsoonal precipitation is observed, followed by decreased precipitation from ~ca. 20.5 to 18 ka BP. The period from ca. ~18 to 15.7 reveals warm and humid climatic conditions. We suggest that a cold event from ca. ~15.7 to 11.5 may correspond to the Younger Dryas (YD) which in turn is followed by a phase of maximum moisture of the Holocene Climate Optimum (HCO) (ca. ~11.5–7.2 ka BP) in the study area. The increased CIA during deglaciation and HCO suggest high chemical weathering, whereas, the LGM (Last Glacial Maximum) and YD are represented by the low CIA. The observed climatic phases/events are in agreement with the records from other parts of the Himalaya.

1. Introduction

The Indian summer monsoon (ISM) or south-west monsoon is an important component of the global climate. The ISM is closely related to the African and East-Asian monsoon systems on millennial time scales (Zhu et al., 1986). During summer (June–September), the South Asian landmass is warmer than the ocean, driving winds from south-west to the north-west towards the continent. In winter (November–February), air over the Asian mainland rapidly cools, creating high atmospheric pressure over continents thus the winds blow from north-west to south-west, forming westerlies (Gupta and Anderson, 2005). The study of Indian Himalaya is important to understand the monsoon dynamics and its interconnection with the global climatic pattern (Bhattacharyya, 1989; Molnar et al., 2010; Ghosh et al., 2015). In general, most of the Quaternary climatic research in the Higher Himalaya is based on glacio-fluvial investigation. However, these studies are limited due to poor preservation of moraine deposits and lack of suitable material for dating (Owen et al., 1997). In such cases, the proglacial lakes in the Higher Himalaya seem good example of valley glaciations as they bear continuous climate record therefore, considered as a reliable archive for palaeoclimatic signatures.

In order to understand the past climate history of the Lahaul Himalaya, we studied an exposed varvite profile from Bharatpur village which is a high altitude region and is less affected by

* Corresponding author.
E-mail address: archna.bohra@gmail.com (A. Bohra).

http://dx.doi.org/10.1016/j.quaint.2017.04.028
1040-6182/

anthropogenic activity. Generally, such sediments have been proved to be good palaeo-environmental archive, bearing climatic signatures of the ISM and Western Disturbances (WDs) (Benn and Owen, 1998; Phartiyal et al., 2009, 2013; 2015; Wünnemann et al., 2008, 2010; Anoop et al., 2013; Leipe et al., 2014a,b; Kramer et al., 2014; Bohra and Kotlia, 2015; Mishra et al., 2015; Kar et al., 2015).

This study attempts to reconstruct the palaeoclimatic changes in the late Pleistocene and Holocene linked to precipitation variability at centennial to millennial scales using geochemical analysis, mineral magnetism and Loss on Ignition (LOI) data from a high altitude palaeo-lake sequence from Bharatpur village near Baralacha Pass (~4900 m a.s.l), upper Lahaul, Himachal Pradesh, NW Himalaya. Various geomorphological features, such as, sinuosity of the Yunam river (Fig. 2a and b), deep gorges and formation of glacial as well as river terraces as top topography is ~30 m above the river bed indicate the tectonic nature of the area (Bohra and Kotlia, 2015). Such features in the tectonic valleys in the Himalaya are very common (e.g., Valdiya and Kotlia, 2001; Joshi and Kotlia, 2015). To generate a regional picture of climate, the palaeoclimatic inferences of the Bharatpur section are compared with the Kilang Sarai section (32° 49′ N: 77° 27′ E, altitude 4573 m a.s.l.), which lies nearly 11 km upstream of Bharatpur section (Figs. 1 and 3) and has been studied by Bohra and Kotlia (2015).

2. Regional setting

2.1. Geology and geomorphology

The Lahaul and Spiti region is located between the Tethyan Himalaya in the north, coinciding with the Indus Tsangpo Suture Zone (Gansser, 1980) whereas the southern boundary is represented by the High Himalayan Crystalline Zone or South Tibetan Detachment System (Searle and Godin, 2003). The two northeast-southeast trending Pir Panjal and the Great Himalaya mountain ranges traverse the Lahaul. The study area Baralacha Pass in Lahaul is located between monsoon influenced southern region and mid latitude westerlies (WDs) in the northern region (Owen et al., 1995). At Baralacha Pass the river Bhaga is flowing southwest direction (in higher Himalaya) and the Yunam River which originates from Baralacha Pass flows towards northeast in eastern Zanskar. The lithology of the area is characterized by presence of phyllite, quartzite, dolomite, shale, schist and limestone of Palaeozoic and Mesozoic age (Bhargava and Bassi, 1998; Bohra and Kotlia, 2015). The region has arid landscape and has been shaped by mountain ranges, vast valleys, high altitude cold deserts, snow clad peaks, freshwater rivers and lakes (Figs. 1–2) and several glacial stages (Owen et al., 1996; Adams et al., 2009; Owen et al., 2001; Bohra et al., 2014; Bohra and Kotlia, 2015; Sharma et al., 2016). The climate of the Lahaul region is cold, semi-arid to arid and the valleys remain covered with snow for nearly six months.

The Geomorphology of the Lahaul region is dominated by glacial and fluvio-glacial deposits of Quaternary period characterized by lacustrine sediments and moraine deposits, preserving records of past glaciations (Owen et al., 1996; Adams et al., 2009; Bohra and Kotlia, 2015). The ^{10}Be Surface exposure dating (SED) of moraine deposits reveal the glacier advance in the Lahaul valley at ~43, 36 and 11 ka BP (Owen et al., 1997) creating the present day geomorphic setting in the region.

2.2. Stratigraphy of Bharatpur sequence

The relict deposits are formed at the terminal moraine at Bharatpur, showing sedimentation in a proglacial situation along Yunam River (see Fig. 1). The exposed section is 6 m thick and has preserved cm to mm scale laminae. Presence of carbonaceous laminae, faulted strata, occasional dropstones and sand layers conform the deposition is not monotonous. The section is divided into three litho-units. The varvite sequence rests on the glacial outwash (~3 m).

Unit 1 (0–65 cm): The lowermost part is greyish carbonaceous mud with prominent light coloured laminations, which at times possess mm to cm scale thick layers of the highly angular gravel (Fig. 3). The sediments are dominantly varvite in nature (Fig. 3) and consist of alternating bundles of laminated ash grey and fine silty horizons.

Unit 2 (65–300 cm): At 65 cm level, a gravel layer is observed and is taken as a marker bed for lateral extension of the sequence. A further continuous gravel layer is noticed 200 cm level. From 200 to 300 cm, the laminated sequence is dominated by sandy mud and clay.

Unit 3 (300–600 cm): This part is dominated by bluish carbonaceous horizons and silty sands with decreasing organic carbon content and from 415 cm onwards, the topmost part is covered by gravel deposit.

3. Sampling and methodology

The exposed profile was sampled at 10 cm interval (Fig. 3). We analyzed 54 samples for geochemistry and magnetic mineralogy. Individual bulk organic samples were dated at Physical Research Laboratory (PRL), Ahmedabad and Institute of Physics (IOP), Bhubaneshwar. All dates were calibrated by using CalPal program. Based on the calibration, four dates were considered for interpretation as, 24.2 ka at 5 cm depth, 21.5 ka at 100 cm, 12.8 ka at 291.5 cm and 12.6 ka at 297 cm (see Table 1). The heterogeneous nature of deposits did not allow us to calculate of the accurate sedimentation rate. Further, suitable dating material for the upper part of the section was not available.

Loss on ignition (LOI) was measured to understand organic content of the sediments (e.g., Bengston and Enell, 1986; Heiri et al., 2001). 5 gm of each sample was combusted at 520 °C step wise temperature at least for 4 h to remove of complete moisture followed by 950 °C. The results are presented in Fig. 4. Geochemical and mineral magnetic proxies were used to obtain a record of possible palaeoenvironmental changes. For major oxides, 5 gm of each bulk powdered sample was added with polyvinyl alcohol. A hydrologic pressure of 2000 kg/cm^2 was given to the mixture to convert it into pellet (~3.5 mm) form. These pellets were measured for major oxides by Philip PW1710 X-ray fluorescence spectrophotometer at Wadia institute of Himalayan Geology, Dehradun. The distribution of major oxides in sediments is thought to be climatically controlled and thus can be used as proxies for palaeoclimatic reconstruction. The major oxides such as Al_2O_3, FeO, Na_2O, CaO, SiO_2 and their intrinsic oxide ratios can be used as proxy of meltwater discharge in the lake (Lisitzin, 1996; Benson et al., 1998) because they are stable in an aqueous regime and are produced by physical weathering in the glacial terrain. An increase in Al_2O_3 is considered as an increase in weathering (Nesbitt and Young, 1984; Selvaraj and Chen, 2006) and high values of Al_2O_3 indicate warm and humid climatic conditions (Newman, 1987). Usually CaO and Na_2O are considered as more soluble and mobile and products of high chemical weathering signifying abundant precipitation. Similarly, Al_2O_3, SiO_2 and Fe_2O_3 are considered as more insoluble and resistant (Mackereth, 1966; Engstrom and Wright, 1984). The ratio of Al_2O_3/SiO_2, Chemical Index of Alteration (CIA) and Chemical Index of Weathering (CIW) were also determined. CIA indicates the changes in the proportion of feldspar and different clay minerals in the weathering product (Nesbitt and Young, 1982). CIA and CIW were calculated using formulae given by

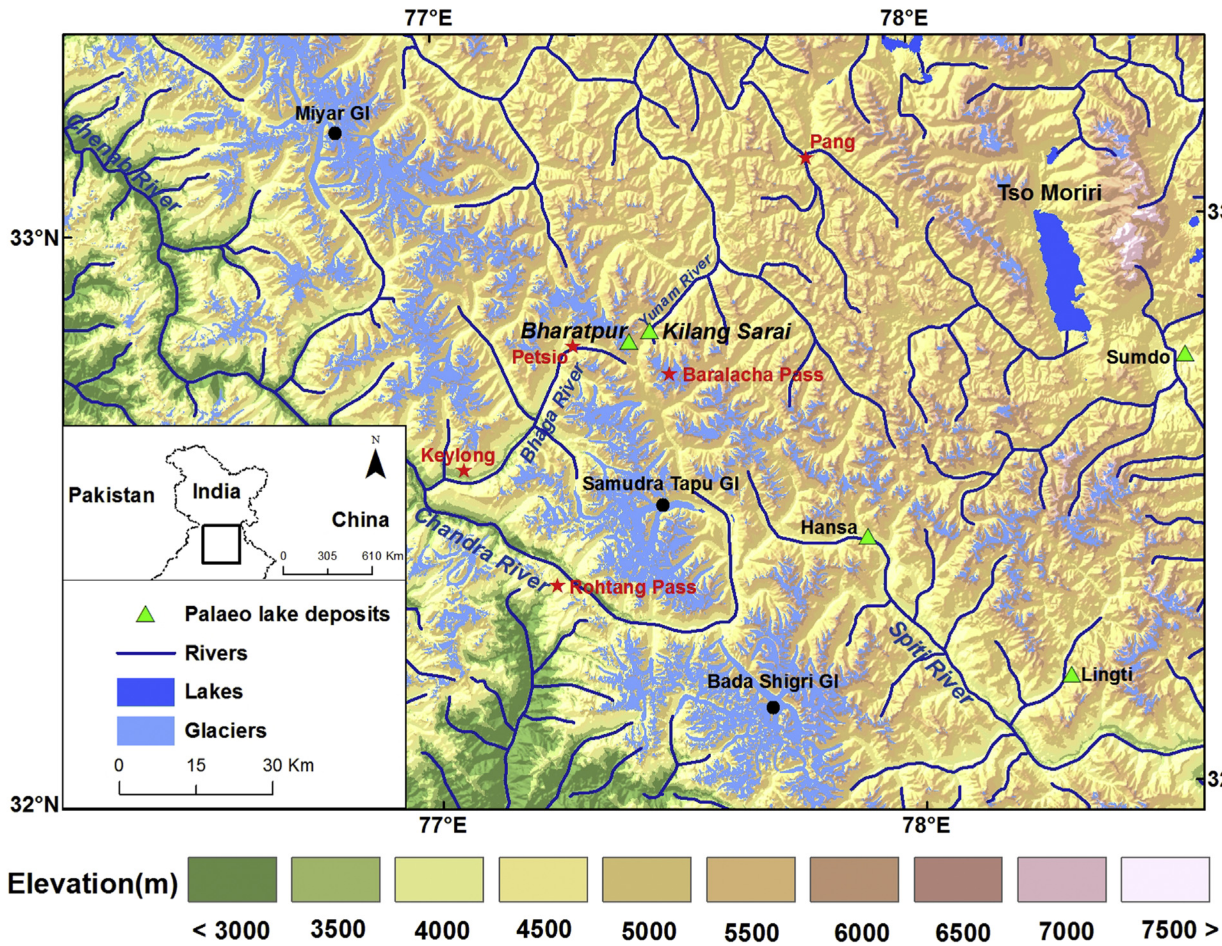

Fig. 1. SRTM image showing the location of study area shown in a rectangle, and a Rivers, Lakes and Glaciers in nearby region in NW Himalaya.

Nesbitt and Young (1982) and Harnois (1988):

$CIA = (Al_2O_3/(Al_2O_3+CaO^*+Na_2O + K_2O) \times 100$; $CIW = (Al_2O_3/(Al_2O_3 + CaO^* + Na_2O) \times 100$

CaO^* is taken in calculation representing the amount of CaO which is incorporated in the silicate fraction of the sediments. In most sediment samples, concentrations of P_2O_5 and $CaCO_3$ are less or absent and therefore the CaO^* concentration can be obtained by using mole ratios of Na_2O and CaO (for details see McLennan, 1993). The Al/Na ratio can be used as weathering index along with CIA and CIW (Figs. 4–5).

Mineral magnetic analysis was carried out using standard techniques and instrumentation at Indian Institute of Geomagnetism, Mumbai (for details see; Bohra and Kotlia, 2015). In this process, we measured response of the material to a range of artificially applied magnetic field. The technique has been applied to various depositional environments (Arkell et al., 1983; Oldfield et al., 1985, 1999; Walden et al., 1995; White et al., 1997; Schmidt et al., 1999; Wheeler et al., 1999; Mooney et al., 2002; Phartiyal et al., 2003; Kotlia et al., 2010). The χ, χARM, χIRM, Soft IRM and ratio derived from them are used to identify variations in the concentration, grain size and mineralogy of the magnetic material (Thompson and Oldfield, 1986; Robinson, 1986; Yu and Oldfield, 1989; King and Channell, 1991). SIRM/χ, χARM/SIRM and χARM/χlf are also calculated for distinguishing different magnetic grain sizes in bulk samples. The low values of SIRM/χ can be ascribed to higher concentrations of these particles. The χARM is sensitive to both concentration and SD grain size therefore normalizing with concentration parameter χlf gives ratio χARM/χlf which can be used for qualitative SD granulometry of bulk samples.

The technique is an interdisciplinary field that utilizes both the natural magnetic remanence and mineral magnetic properties of natural materials to study the process and structure of environmental systems. This is because, magnetic minerals, particularly iron oxides occur more or less universally, iron being elements in the earth's crust. They may be present in minor amounts, usually <1%, but they are easily, rapidly and nondestructively detected.

4. Results and interpretation

Various data on the chronology, geochemistry and mineral magnetism are discussed below;

4.1. Chronology

The Chronology is based on ^{14}C dates bulk sediments samples is shown in Table 1. By extrapolating the dates (Table 1), we assume that the average sedimentation rates vary from 45.07cm/ka for the period ~12.6–21.5 ka BP to 28.9 cm/ka for the period between ~21.5 and ~24.3 ka BP. Considering this, the basement of the profile may be approximated as ca. 24.3 ka BP. The age of different climatic boundaries are 24.3 ka BP (5 cm level), ~21.5 ka BP (100 cm level),

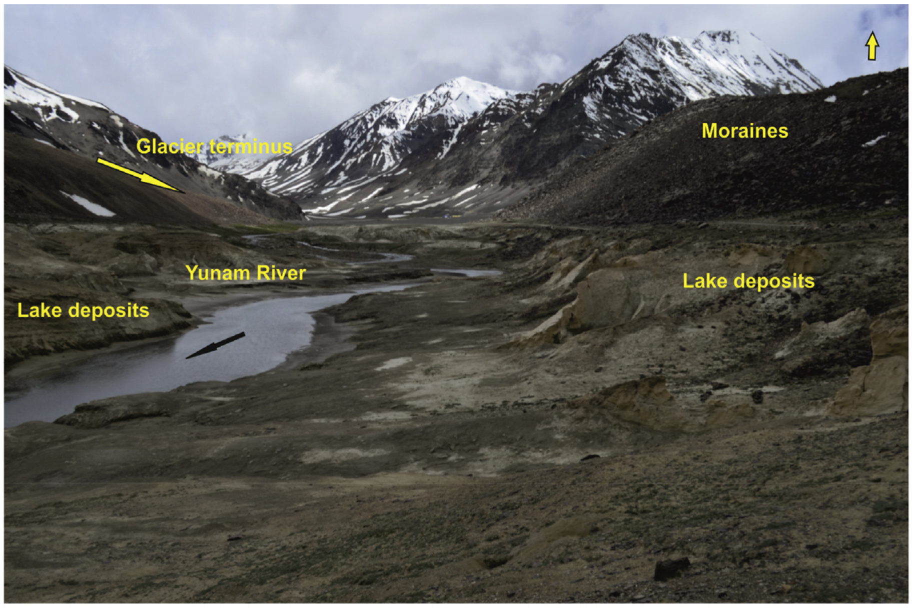

Fig. 2. Panoramic view of Bharatpur showing different topographic structures.

~12.8 ka BP (291.5 cm) and 12.6 ka BP (297 cm) (see Table 1).

4.2. Geochemical and magnetic mineralogy

On the basis of geochemical and magnetic analyses, six climatic zones can be identified in the Bharatpur profile (Figs. 4–5) and a possible palaeoclimate picture can be visualized zone-wise as below.

4.2.1. Zone-1 (0–60 cm, ca. 24.3–22.6 ka BP)

This zone is characterized by various ranges of values such as CIA (61.68–66.0), LOI (5.6–6.23), Fe_2O_3 (0.034–0.037), MgO (0.04–0.05), CaO (0.027–0.036%), CIW (77.62–84.88), Al_2O_3/SiO_2 (0.002–0.003), χ (0.97–1.01) and χfd% (1.21–2.05%).

4.2.2. Zone-2 (60–120 cm, ca. 22.6–20.5 ka BP)

The zone is specified by slightly higher values of CIA (62.21–66), CIW (78.18–84.88), Al_2O_3/SiO_2(0.035–0.04%) and average low values of CaO (0.027–0.037%), as compared to preceding zone.

4.2.3. Zone-3 (120–160 cm, ca. 20.5–18 ka BP)

This period is characterized by considerably low values of LOI

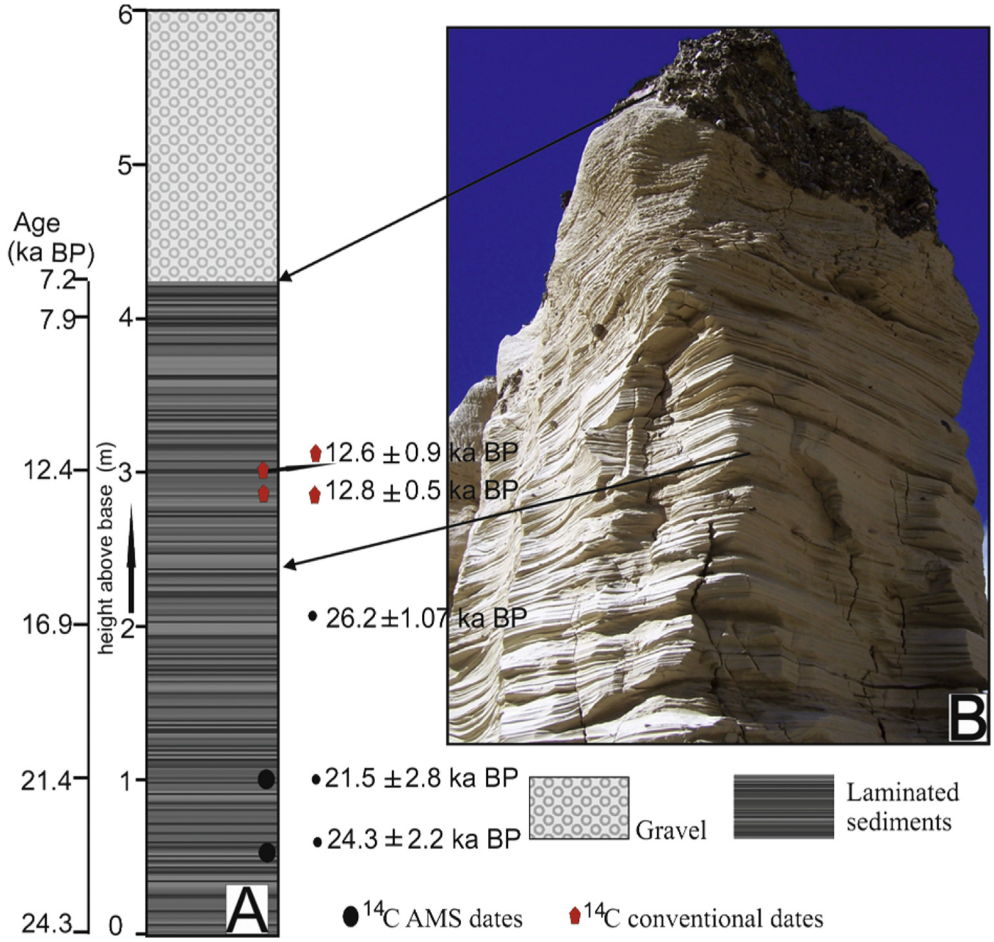

Fig. 3. a). Detailed litholog of the Bharatpur sequence with identified lithologies and radiocarbon dates b). Close view of the laminated sediments.

Table 1
Radiocarbon dates of Bharatpur varvite samples.

Lab number	Depth (m)	Sample type	14C age calibrated	Difference between two ages (depth wise)	Sedimentation rate (cm/ka)
PRL-3166	297	bulk sediment	12,600 ± 900	8880	45.07
PRL-3165	291.5	bulk sediment	12,800 ± 500		
IOP-711	100	bulk sediment	21,480 ± 2800	2750	28.95
IOP-710	5	bulk sediment	24,230 ± 2200		
	calibration by on-line Cal Pal program				

(5.18–5.83%), CIA (62.48–65.26), CIW (77.69–82.99), χfd% (1.52–1.69), χ (0.96–0.99), χARM/χ, χARM/SIRM, Fe_2O_3 (0.034–0.37%) and high values of CaO (0.003–0.004%).

4.2.4. Zone-4 (160–230 cm, ca. 18–15.7 ka BP)

This time period is represented by higher values of LOI (5.18–6.87%), CIA (>65.09), CIW (82.28–84.5), χ (0.99–1.00), χARM/χ, χARM/SIRM, and low values of MgO (0.052–0.06%), CaO (0.027–0.031%) and approximately similar values of Fe_2O_3 (0.035–0.038%) and Al_2O_3/SiO_2 as compared to preceding zone (Figs. 4 and 5).

4.2.5. Zone-5 (230–310 cm, ca. 15.7–11.5 ka BP)

This zone is characterized by decreasing trend in values of CIA (62.49–67.37), CIW (77.89–84.04), Al_2O_3/SiO_2, Fe_2O_3 (0.035–0.040), χ (0.94–1) χARM/χ, and slight increase in CaO (0.028–0.043) and MgO (0.052–0.057) (Figs. 4–5).

4.2.6. Zone-6 (310–410 cm, ca. 11.5–7.2 ka BP)

This zone is represented by relatively higher values of CIA (64.36–67.12), CIW (80.54–85.62), Al_2O_3/SiO_2 (0–002.0.003), χfd (1.82–2.62%), χ (0.62–0.98), χARM/χ, χARM/SIRM, Fe_2O_3 (0.035–0.039) and lower values of CaO (0.024–0.034) and SIRM/χ (Figs. 4–5).

5. Discussion

The 6 m thick varvite sequence at Bharatpur provides a likely climatic record of ~24.3–7.2 ka BP. The data show that the sequence bears moderate kind of weathering due to low values of Al/Na ratio, suggesting presence of small amounts of Na_2O (plagioclase) in the sample. It can be observed that Al/Na ratio is more variable than the CIA and CIW (Fig. 4). The lowest Al/Na ratio can be observed during the LGM part (~20.5–17.5 ka BP), YD (~15.7–11.5 ka BP) and increasing ratio in deglacial (~18.7–15.7 ka BP) and Holocene

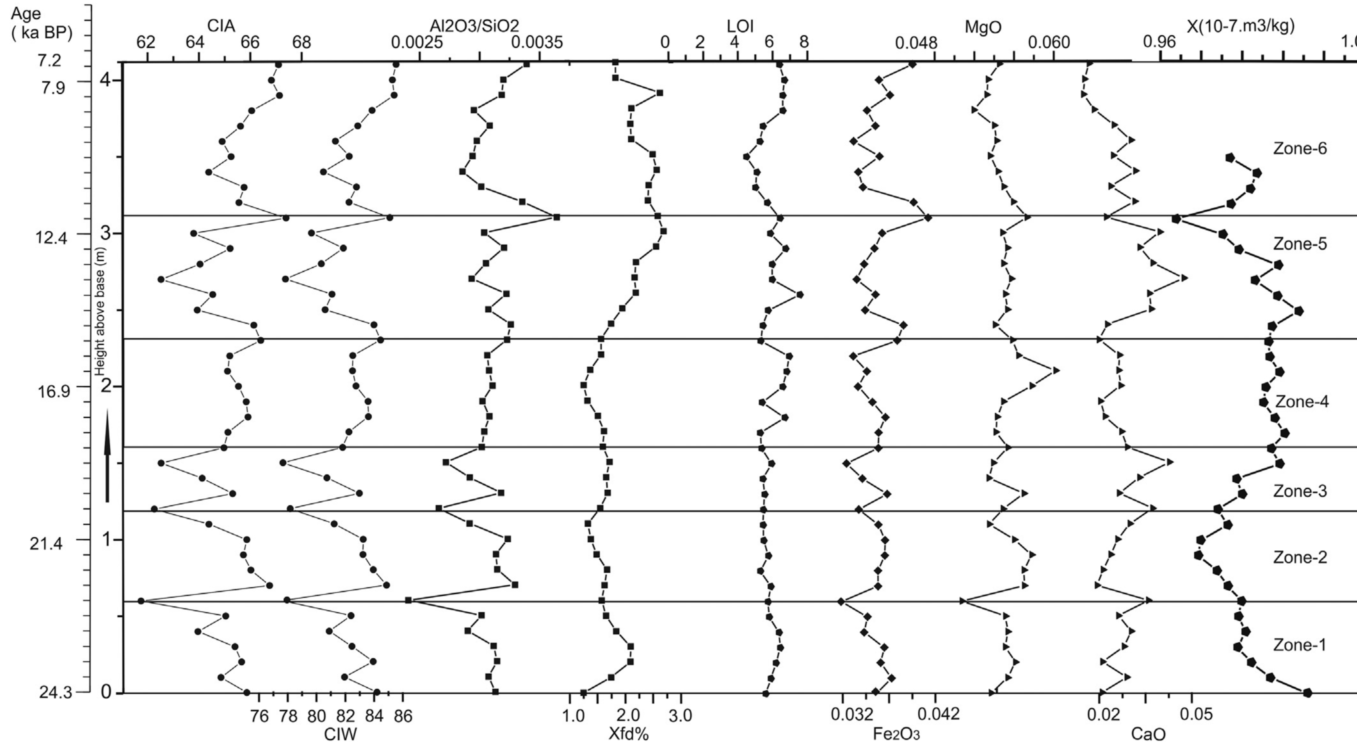

Fig. 4. Concentration of various elements, oxides and magnetic parameters, plotted against litholog and ages.

intervals (~9.8–7.2 ka BP). The higher ratios of major oxides indicate more input of soluble and mobile elements into Bharatpur lake during intervals of prominent hydroclimatic regime in the catchment and hence intense chemical weathering conditions.

Six climatic phases have been identified during the period of sedimentation. This profile seems to be a part of Kilang Sarai lacustrine section (Bohra and Kotlia, 2015) which is 11 km far from Bharatpur section. The Kilang Sarai profile bears a palaeoclimatic record of 25-2 ka BP with eight climatic zones as has been described by Bohra and Kotlia (2015). A comparison of these climatic phases (unit 1 to unit 8) marked by Bohra and Kotlia (2015), gives a clear picture of correlation with Bharatpur data (zone1 to zone6) (Fig. 6). The sedimentary record of Bharatpur shows prominent cold and warm phases with aridity between ~ ca. 24.3 and 22.6 ka. From ~ ca. 22.6–20.5 ka BP, a slight increase in monsoon and subsequently an arid phase from ~ca. 20.5 to 18 ka BP can be established. A climatic amelioration is observed from ca. ~18–15.7 ka BP which is followed by of the YD event around 15.7–11.5 ka BP. This perhaps can be related to stronger influence of WDs and weak summer monsoon. In our results, a period from ca. ~11.5–7.2 ka BP indicates warmest phase in the Upper Lahaul Himalaya.

5.1. *ca. 24.3–22.6 ka BP*

This time bracket signifies the low values of LOI indicating poor development of vegetation under reduced precipitation. This may also have affected the water budget of the lake which may have been oligotrophic during this period. The high CaO values, and low CIA, CIW and Al_2O_3/SiO_2 (Fig. 5) reveal the absence of chemical alteration, corresponding to the sedimentation under glacial conditions that may reflect cool and arid conditions. The decreasing trend in χ and χ_{ARM}/χ is possibly due to a decrease in precipitation under anoxic mineral phase.

5.2. *ca. 22.6–20.5 ka BP*

The higher values of CIA, CIW, Al_2O_3/SiO_2 ratio and Al/Na (Fig. 4) but low values of CaO and MgO possibly indicate intense weathering conditions in the catchment. The results are further supported by magnetic data which shows high values of χ and χfd suggesting input of finer grained material under high rainfall owing to warm and humid climatic conditions. Similarly, Kilang Sarai in nearby area witnessed climatic amelioration at ca. 23-19 ka with lower δ^{13}C and higher susceptibly values (Bohra and Kotlia, 2015). Intensification of monsoon around 22.0 ka BP is also recorded from the Indus valley (Sharma et al., 1998), Tibet (Yan et al., 1999), Kumaun Himalaya (Kotlia et al., 2000), Africa and Atlantic sea cores (Bonnefille and Riollet, 1988).

5.3. *ca. 20.5–18 ka BP*

Our record indicates reduction in the mass deposition of inorganic material caused by highly erosive conditions in the catchment. Thus, the low LOI may indicate less input of organic content under the oligotrophic conditions. It is further supplemented by a shift in MgO, CaO, CIA and CIW, showing positive correlation. Our results may suggest reduced melt water under cold/arid conditions. We observed a good correlation with 18.3 ka arid event manifested by pollen results from the Tsokar Lake in Ladakh (Bhattacharyya, 1989). Similarly, Central Himalaya experienced an arid phase during the LGM between 28 and 18 ka (Kotlia et al., 1997, 2000, 2010; Owen et al., 2002; Basavaiah et al., 2004), as well as Nepal Himalaya during 25-18 ka (Richards et al., 2001) and its peak (ca. 18 ka BP) in north-eastern Tibetan Plateau (Yan et al., 1999) is marked by cold and a dry climate and drop of 1200 m in the upper limit of timberline in western China (Liang et al., 1990). The glaciers of Garhwal Himalaya advanced about 40 km beyond their present ice fronts (Owen et al., 2002) and occupied expanded positions at ca.

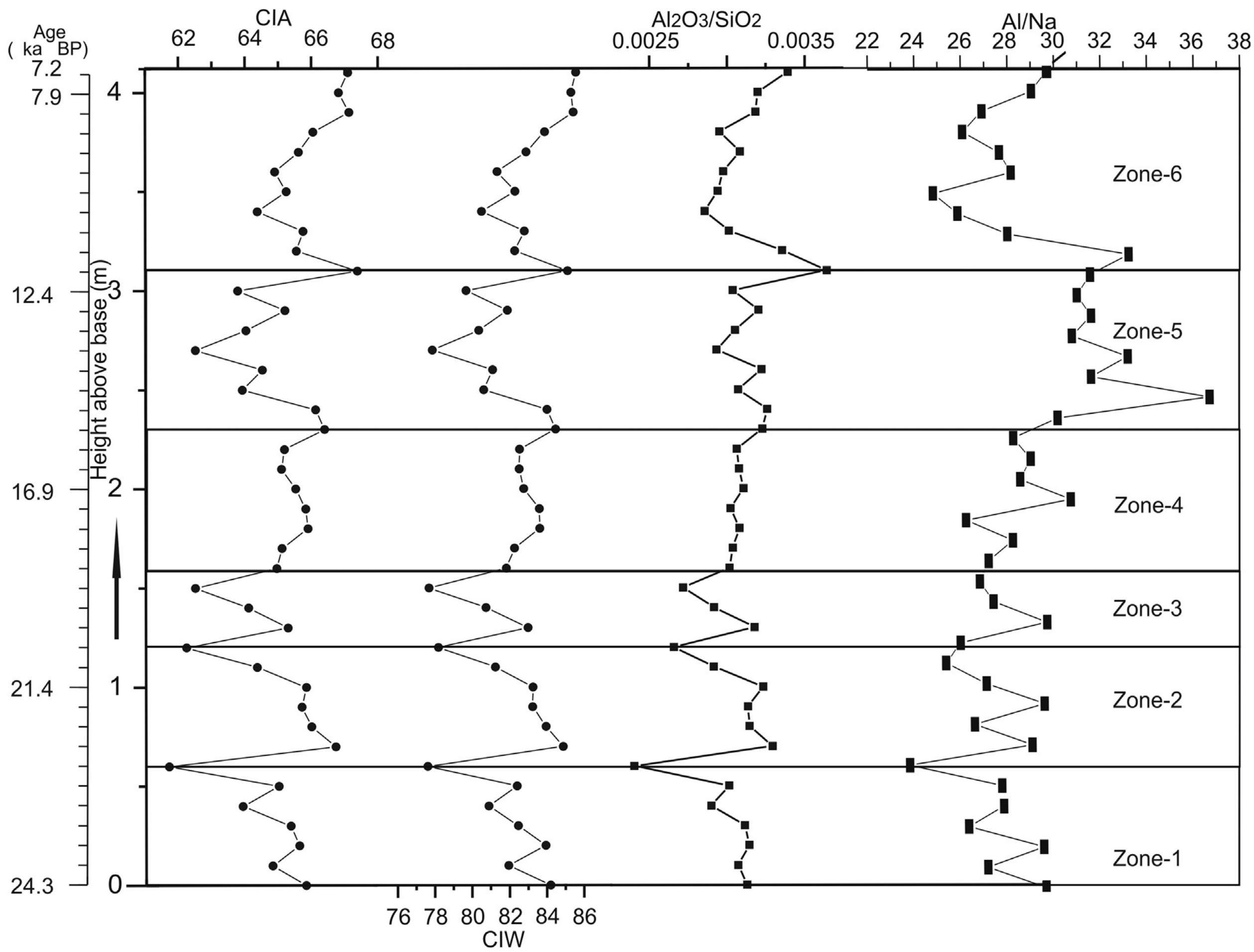

Fig. 5. Comparison of Al_2O3/SiO_2, Chemical Index of alteration (CIA), Chemical Index of weathering (CIW) and Al/Na ratio.

18.0 ka BP (Benn and Owen, 1998). A number of other north Himalayan Glaciers reached their maximum positions at 22-18 ka BP (Benn and Owen, 1998).

5.4. *ca. 18–15.7 ka BP*

During this time bracket, the Bharatpur sequence registers climatic amelioration, as is evident by high values of LOI possibly due to more input of the clastic sediments and good drainage under wetter conditions. The increasing trend in Al_2O_3/SiO_2 points to gradual increase in weathering, indicating higher precipitation. The results are in agreement with high CIA as well as CIW (Figs. 4–5), indicating mineral formation under intense weathering which may be suggestive of warm/humid climatic conditions in the catchment area. Similarly, increasing trend in χ, χARM/SIRM, χARM/χ and Fe_2O_3 shows finer grained material with higher concentration of pedogenic magnetite minerals which may suggest high rainfall conditions under favourable conditions. This interval of climatic amelioration is in agreement with palaeoclimatic data of NW Himalaya, e.g., a deglaciation is witnessed at ca. 15 ka BP (Singh and Agrawal, 1976); a prominent phase of climatic amelioration was established at 15.8 ka BP in Ladakh (Bhattacharyya, 1989). Similarly, the post-glacial temperatures started to rise around this time in Tibetan Plateau (Yan et al., 1999; Zhang and Mischke, 2009) and climatic amelioration took place with higher susceptibility signatures in China between ca. 18 and 15 ka BP (Feng et al., 2007).

5.5. *ca. 15.7–11.5 ka BP*

During this time period, low values of CIA, CIW, Al_2O_3/SiO_2, Fe_2O_3, χ and χARM/χ indicate a strong hydrodynamics and poor chemical weathering under reduced precipitation. Slightly increased values of CaO and MgO point towards reduction in the lake level with reduced surface erosion. In south western Tibet, the dry climatic conditions are also recorded in pollen records at around 12 ka and prior to ca. 11 ka BP in the Pangong Co region (Van Campo and Gasse, 1993; Van Campo et al., 1996), Central Asia (Herzschuh, 2006) and also the glacier advancement at 15.1–12 ka BP in Lahaul (Owen et al., 1997) and during 16-12 ka BP in Zanskar valley (Taylor and Mitchell, 2000). However, the data from the Kumaun Higher Himalaya indicate the inception of the OD at around 14.5 ka-13.8 ka BP (Kotlia and Joshi, 2013).

5.6. *ca. 11.5–7.2 ka BP*

During this time span, our data show increased weathering conditions with high CIA, CIW and Al_2O_3/SiO_2 under wetter/moist regime. The mineral magnetic data (high χfd, χ, χARM/SIRM, χARM/χ) and low CaO, MgO and SIRM/χ also confirm our observations. These reflect wet climate with high monsoon precipitation resulting in relative high melt-water discharge consistent with higher lake level. This onset of Indian summer monsoon could be related to a small southward shifting of ITCZ and can be comparable with interglacial around 11.2–8.5 ka BP (Schulz et al., 1998; Wang

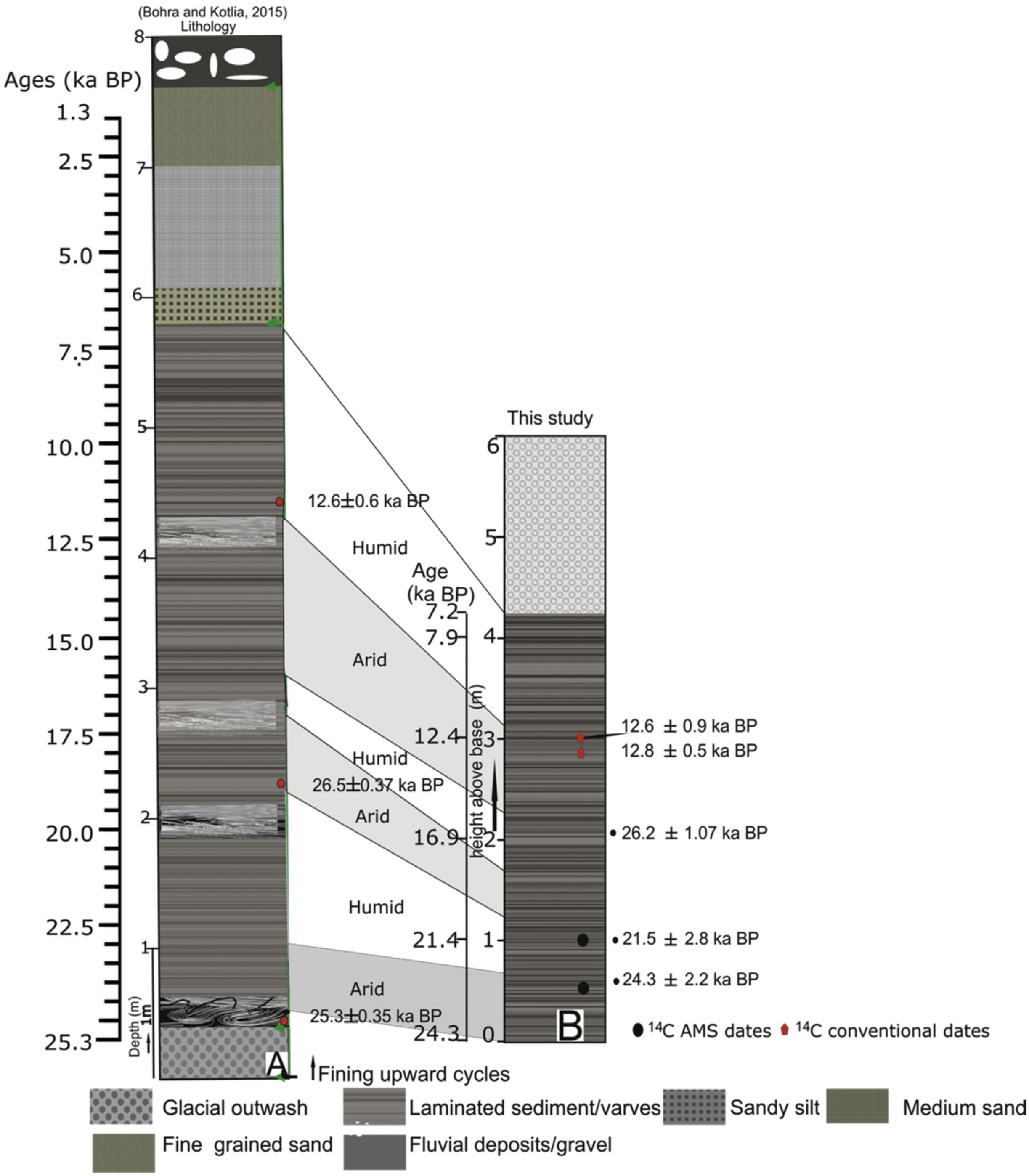

Fig. 6. Multi-proxy results in the present study is in harmony with climatic events observed in the Kilang Sarai profile.

et al., 2001; Yuan et al., 2004) and which may have led to penetration of ISM in the study region (e.g., Sinha et al., 2005) during warm and humid interval. Our results are in agreement with several palaeoclimatic records of western Tibet and Karakoram around ca. 11.5 ka BP (Brown et al., 2003), Tsokar and Tso Moriri in Ladakh (Fontes et al., 1993; Demske et al., 2009; Wünnemann et al., 2008, 2010; Leipe et al., 2014a,b), Kilang Sarai in upper Lahaul (Bohra and Kotlia, 2015), Chandra Tal Lake in Spiti (Rawat et al., 2015) and Sumxi Co, Bangong Co and Quidam Basin in Tibet (Van Campo and Gasse, 1993; Van Campo et al., 1996; Hui et al., 1996; Zhao et al., 2007; Herzschuh, 2006; Mischke and Zhang, 2010; Dietze et al., 2013; Doberschütz et al., 2014). At Sumxi Co, the wet conditions were established around 11.5 ka BP with a humid interval lasting until ca. 8.8 ka BP (Van Campo and Gasse, 1993). Both the intensity and seasonal length of the summer monsoon increased when the Himalaya and Tibetan Plateau became warmer and the summer insolation maximum reached the lower latitudes at ca. 10 ka BP. This is in agreement with the initiation of enhanced monsoon and onset of humid environment from ca. 11.5 ka BP onwards in western Tibet and Karakoram (Brown et al., 2003). In slightly higher latitudes, the Tibetan Plateau experienced onset of Holocene warming between ca. 10 and 9.4 ka BP (Yan et al., 1999). In western Tibet, warm/wet conditions, attributed to the monsoon influence, were established at ca. 9.6 ka BP (Fontes et al., 1996) and a clear cut warm pulse with increased A/C ratio, ostracod content and TOC is observed between ca. 10-8 ka BP (Gasse et al., 1991). The Bangong lake had the highest water level around ca. 9.6–8.7 ka BP (Hui et al., 1996) and the moisture conditions prevailed until ca. 6.2 ka BP (Van Campo et al., 1996). Thus, most multi-proxy data in several Tibetan lakes show humid pulse from ca. 10 ka BP onwards indicating improved monsoon circulation (Fontes et al., 1993; Van Campo and Gasse, 1993). The moisture availability strongly increased in the Lake Koucha region in Tibetan Plateau at about 7.3 ka BP (Mischke and Zhang, 2010).

6. Conclusion

The geomorphological, geochemical and mineral magnetic investigations in the Bharatpur varvite sequence in NW India provide a climatic record of ~ca. 24.3 to 7.2 ka BP, which gives the continuity of sedimentation process from Late Quaternary to Early Holocene. Six climatic phases have been identified during the period of varvite sedimentation. The period between ~ ca. 24.3 and 22.6 ka can be regarded as an arid climatic condition. From ~ ca. 22.6 to 20.5 ka BP, a slight increase in precipitation is observed followed by decrease in monsoon during ~ca. 20.5–18 ka BP. A period from 18 to 15.7 ka BP a warm and humid climatic episode followed by an arid phase from 15.7 to 11.5, corresponding to the Younger Dryas (YD). A period from ca. ~11.5–7.2 ka BP indicates Holocene Climate Optimum (HCO) in the Upper Lahaul Himalaya.

Acknowledgements

AB acknowledges the support of SERB-DST Govt. of India under Fast Track Young Scientist Project (research grant #SR/FTP/ES-114/2012) and is thankful to the Prof. Anil K. Gupta, Director, Wadia Institute of Himalayan Geology, Dehradun and to Dr. D.P. Dobhal for constant encouragement and support. BSK is thankful to the Ministry of Earth Sciences (MoES/PO/43/2015), New Delhi for financial support. We thank the Director, Institute of Geomagnetism, Mumbai for providing facilities for mineral magnetic measurements and to R Ramesh and MG Yadava, PRL, Ahmadabad for radiocarbon dates. We are highly grateful to three anonymous reviewers for their critical suggestions which highly improved this manuscript.

References

Adams, B., Dietsch, C., Owen, L.A., Caffee, M.W., Spotila, J., Haneberg, W.C., 2009. Exhumation and incision history of the Lahaul Himalaya, northern India, based on (UeTh)/He thermochronometry and terrestrial cosmogenic nuclide methods. Geomorphology 107 (3), 285–299.
Anoop, A., Prasad, S., Krishnan, R., Naumann, R., Dulski, P., 2013. Intensified monsoon and spatiotemporal changes in precipitation patterns in the NW Himalaya during the early–mid Holocene. Quat. Int. 313–314, 74–84.
Arkell, B., Leeks, G., Newson, M., Oldfield, F., 1983. Trapping and tracing: some recent observations of supply and transport of coarse sediment from upland Wales. Special Publ. Int. Assoc. Sedimentol. 6, 107–119.
Basavaiah, N., Juyal, N., Pant, R.K., Yadava, M.G., Singhvi, A.K., Appel, E., 2004. Late Quaternary climatic changes reconstructed from mineral magnetic studies from proglacial lake deposits of Higher Central Himalaya. J. Indian Geophys. Union 8 (1), 27–37.
Bengston, L., Enell, M., 1986. Chemical analysis. In: Berglund, B.E. (Ed.), Handbook of Holocene Palaeoecology and Palaeohydrology. John Wiley, New York, pp. 423–451.
Bhargava, O.N., Bassi, U.K., 1998. Geology of Spiti-Kinnaur, Himachal Himalaya. Geol. Surv. India Memo. 124, 1–210.
Benn, D.I., Owen, L.A., 1998. The role of the Indian summer monsoon and the mid-latitude westerlies in Himalayan glaciations: review and speculative discussion. J. Geol. Soc. 155, 353–363.
Benson, L.V., May, H.M., Antweiler, R.C., Brinton, T.I., 1998. Continuous lake-sediment record of glaciation in Siera Nevada between 12,500 14C Yr B.P. Quat. Res. 50, 113–127.
Bhattacharyya, A., 1989. Vegetation and climate during the last 30,000 years in Ladakh. Palaeogeogr. Palaeoclimatol. Palaeoecol. 73, 25–38.
Bohra, A., Kotlia, B.S., 2015. Tectono-climatic signatures during the Late Quaternary in the Yunam Basin, Baralacha Pass (Upper Lahaul Valley, India), derived from multi-proxy records. Quat. Int. 371, 111–121.
Bohra, A., Kotlia, B.S., Laskar, A.H., Yadava, M.G., 2014. Evidence of late Quaternary seismicity from Yunam Tso, Lahaul and Spiti, NW Himalaya India. J. Earth Syst. Sci. 123 (3), 603–616.
Bonnefille, R., Riollet, G., 1988. The Kashiru pollen sequence (Burundi). Palaeoclimatic implications for the last 40,000 yr B.P. in tropical Africa. Quat. Res. 30, 19–35.
Brown, E.T., Bendick, R., Bourles, D.L., Gaur, V., Molnar, P., Raisbeck, G.M., Yiou, F., 2003. Early Holocene climatic record in geomorphological features in western Tibet. Palaeogeogr. Palaeoclimatol. Palaeoecol. 199, 141–151.
Demske, D., Tarasov, P.E., Wünnemann, B., Riedel, F., 2009. Late glacial and Holocene vegetation, Indian monsoon and westerly circulation dynamics in the Trans-Himalaya recorded in the pollen profile from high-altitude Tso Kar Lake, Ladakh N-W India. Palaeogeogr. Palaeoclimatol. Palaeoecol. 279 (3–4), 172–185.
Dietze, E., Wünnemann, B., Hartmann, K., Diekmann, B., Jin, H., Stauch, G., Yang, S., Lehmkuhl, F., 2013. Early to mid-Holocene lake high-stand sediments at Lake Donggi Cona, northeastern Tibetan Plateau, China. Quat. Res. 79, 325–336.
Doberschütz, S., Frenzel, P., Haberzettl, T., Kasper, T., Wang, J., Zhu, L., Daut, G., Schwalb, A., M€ausbacher, R., 2014. Monsoonal forcing of Holocene paleoenvironmental change on the central Tibetan Plateau inferred using a sediment record from Lake Nam Co (Xizang, China). J. Paleolimnol. 51, 253–266.
Engstrom, D.R., Wright, H.E., 1984. Chemical stratigraphy of lake sediments as record of environmental change. In: Haworth, E.Y., Lund, J.W.G., Lind (Eds.), Lake Sediments and Environmental History. Leicester University Press, pp. 11–67.
Feng, D.Z., Zhai, X.W., Ma, Y.Z., Huang, C.Q., Wang, W.G., Zhang, H.C., Khosbayar, P., Narantseteg, T., Liu, K.B., Rutter, N.W., 2007. Aeolian environmental change in the northern Mongolian plateau during the past ~35,000 yr. Palaeogeogr. Palaeoclimatol. Palaeoecol. 245, 505–517.
Fontes, J.Ch., Mélières, F., Gibert, E., Liu, Q., Gasse, F., 1993. Stable isotope and radiocarbon balances of two Tibetan lakes (Sumxi Co and Longmu Co) from 13,000 yr B.P. Quat. Sci. Rev. 12, 875–887.
Fontes, J.C., Gasse, F., Gibert, E., 1996. Holocene environmental changes in lake Bangong basin (western Tibet). Part 1: chronology and stable isotopes of carbonates of a Holocene lacustrine core. Palaeogeogr. Palaeoclimatol. Palaeoecol. 120, 25–47.
Gansser, A., 1980. The significance of the Himalayan suture zone. Tectonophysics 62 (1–2), 40–50.
Gasse, F., Arnold, J.C., Fontes, M., Fort, E., Gibert, A., Huc, L., Bingyan, L., Yuanfang, L., Qing, F., Melieres, E., Van Campo, Fubao, Q.Z., 1991. A 13.000-Year climate record from western Tibet. Nature 353, 742–745.
Ghosh, R., Bera, S., Sarkar, A., Paruya, D.K., Yao, Y.F., Li, C.S., 2015. A ~50 ka record of monsoonal variability in the Darjeeling foothill region, eastern Himalayas. Quat. Sci. Rev. 114, 100–115.
Gupta, A.K., Anderson, D.M., 2005. Mysteries of the Indian ocean monsoon system. J. Geol. Soc. India 65, 54–60.
Harnois, L., 1988. The CIW index: a new chemical index of weathering. Sediment. Geol. 55, 31–32.
Heiri, O., Lotter, A.F., Lemcke, G., 2001. Loss on Ignition as a method for estimating organic and carbonate content in sediment; reproducibility and comparability of results. J. Paleolimnol. 25, 101–110.
Herzschuh, U., 2006. Palaeo-moisture evolution in monsoonal Central Asia during the last 50,000 years. Quat. Sci. Rev. 25, 163–178.
Hui, F., Gasse, F., Huc, A., Yuanfang, L., Sifeddine, A., Soulie-Marsche, I., 1996. Holocene environmental changes in Bangong Co basin (Western Tibet). Part 3: biogenic remains. Paleogeogr. Paleoclimatol. Paleoecol. 120, 65–78.
Joshi, L.M., Kotlia, B.S., 2015. Neotectonically triggered instability around the palaeolake regime in Central Kumaun Himalaya, India. Quat. Int. 371, 219–231.
Kar, R., Bajpai, R., Singh, A.D., 2015. Modern pollen assemblages from Hamtah and Chhatru glaciers, Lahaul-Spiti, India: Implications for pollen-vegetation relationship in an alpine arid region of western Himalaya. Quat. Int. http://dx.doi.org/10.1016/JQuaint201502 047.
King, J.W., Channell, J.E.T., 1991. Sedimentary magnetism, environmental magnetism and magnetostratigraphy. Rev. Geophys. 358–370.
Kotlia, B.S., Bhalla, M.S., Sharma, C., Ramesh, R., Rajagopalan, G., Mathur, P.D., Bhandari, S., Chacko, S.T., 1997. Palaeoclimatic conditions in the Upper Pleistocene and Holocene Bhimtal-Naukuchiatal lake Basin in the South-central Kumaun, north India. Palaeogeogr. Palaeoclimatol. Palaeoecol. 130, 307–322.
Kotlia, B.S., Joshi, L.M., 2013. Neotectonic and climatic impressions in the zone of Trans Himadri Fault (THF), Kumaun Tethys Himalaya (India): a case study from palaeolake deposits. Z. fur Geomorphol. 57 (3), 289–303. http://dx.doi.org/10.1127/0372-8854/2013/0057-0101.
Kotlia, B.S., Sanwal, J., Phartiyal, B., Joshi, L.M., Trivedi, A., Sharma, C., 2010. Late Quaternary climatic changes in the eastern Kumaun Himalaya, India, as deduced from multi-proxy studies. Quat. Int. 213, 44–55.
Kotlia, B.S., Sharma, C., Bhalla, M.S., Rajagopalan, G., Subrahmanyam, K., Bhattacharyya, A., Valdiya, K.S., 2000. Palaeoclimatic conditions in the Late Pleistocene Wadda lake, eastern Kumaun Himalaya (India). Palaeogeogr. Palaeoclimatol. Palaeoecol. 162, 105–118.
Kramer, M., Kotlia, B.S., Wünnemann, B., 2014. A Late Quaternary ostracod record from the Tso Kar basin (North India) with a note on the distribution of Recent

species. J. Palaeolimnol. 51, 549–565.
Leipe, C., Demske, D., Tarasov, P.E., 2014a. A Holocene pollen record from the northwestern Himalayan lake Tso Moriri: implications for palaeoclimatic and archaeological research. Quat. Int. 348, 93–112.
Leipe, C., Demske, D., Tarasov, P.E., Wünnemann, B., Riedel, F., 2014b. Potential of pollen and non-pollen palynomorph records from Tso Moriri (Trans-Himalaya, NW India) for reconstructing Holocene limnology and human-environmental interactions. Quat. Int. 348, 113–129.
Liang, H.C., Su, Y.M., Qian, W.X., 1990. Preliminary Study on Minor Climate in Montane Areas. Western Sichuan Press of Science and Technology, Chengdu, pp. 85–107.
Lisitzin, A.P., 1996. The age of terrigenous material as an indicator of its origins (age and isotopic measurements) oceanic sedimentation, lithology and geochemistry. Am. Geophys. Union Publ. 192–230.
Mackereth, F.J.H., 1966. Some chemical observations of post-glacial lake sediments. Proc. R. Soc. B 250, 165–213.
McLennan, M., 1993. Weathering and global denudation. Geology 101, 295–303.
Mischke, S., Zhang, C., 2010. Holocene cold events on the Tibetan Plateau. Glob. Planet. Change 72, 155–163.
Mishra, P.K., Anoop, A., Schettler, G., Prasad, S., Jehangir, A., Menzel, P., Naumann, R., Yousuf, A.R., Basavaiah, N., Deenadayalan, K., Wiesner, M.G., Gaye, B., 2015. Reconstructed late Quaternary hydrological changes from Lake Tso Moriri, NW Himalaya. Quat. Int. 371, 76–86.
Molnar, P., Boos, W.R., Battisti, D.S., 2010. Orographic controls on climate and paleoclimate of Asia: thermal and mechanical roles for the Tibetan Plateau. Annu. Rev. Earth Planet. Sci. 38 (1), 77.
Mooney, S.D., Geiss, C., Smith, M.A., 2002. The use of mineral magnetic parameters to characterize archaeological ochres. J. Archaeol. Sci. 29 http://dx.doi.org/10.1006/jasc.2002.0856.
Nesbitt, H.W., Young, G.M., 1982. Early Proterozoic climates and plate motions inferred from major element chemistry of Lutites. Nature 299, 715–717.
Nesbitt, H.W., Young, G.M., 1984. Prediction of some weathering trends of plutonic and volcanic rocks based on thermodynamic and kinetic considerations. Geochem. Cosmochim. Acta 48, 1523–1534.
Newman, A.C.D., 1987. Chemistry of clay and clay minerals. In: Mineralogical Society Monograph, vol. 6, p. 480.
Oldfield, F., Appleby, P.G., Van der Post, K.D., 1999. Problems of core correlation, sediment source ascription and yield estimation in Ponsonby Tarn, West Cumbria, UK. Earth Surf. Process. 24, 975–992.
Oldfield, F., Maher, B.A., Donoghue, J., Pierce, J., 1985. Particle size related, mineral magnetic source sediment linkages in the Rhode River catchment, Maryland, USA. J. Geol. Soc. Lond. 142, 1035–1046.
Owen, L.A., Bailey, R.M., Rhodes, E.J., Mitchell, W.A., Coxon, P., 1997. Style and timing of glaciation in the Lahul Himalaya, northern India: a framework for reconstructing late Quaternary palaeoclimatic change in the western Himalayas. J. Quat. Sci. 12, 83–109.
Owen, L.A., Benn, D.I., Derbyshire, E., Evans, D.J.A., Mitchell, W.A., Thompson, D., Richardson, S., Lloyd, M., Holden, C., 1995. The geomorphology and landscape evolution of the Lahaul Himalaya northern India. Geomorphology 39 (2), 145–174.
Owen, L.A., Derbyshire, E., Richardson, S., Benn, D.I., Evans, D.J.A., Mitchell, W.A., 1996. The quaternary glacial history of the Lahul Himalaya, northern India. J. Quat. Sci. 11, 25–42.
Owen, L.A., Finkel, R.C., Caffee, M.W., Gualtieri, L., 2002. Timing of multiple late Quaternary glaciations in the Hunza Valley, Karakoram Mountains, northern Pakistan: defined by cosmogenic radionuclide dating of moraines. Geol. Soc. Am. Bull. 114 (5), 593–604.
Owen, L.A., Gualtieri, L., Finkel, R.C., Caffee, M.W., Benn, D.I., Sharma, M.C., 2001. Cosmogenic radionuclide dating of glacial landforms in the Lahaul Himalaya, northern India: defining the timing of Late Quaternary glaciations. Quat. Sci. 16 (6), 555–563.
Phartiyal, B., Appel, A., Blaha, U., Hoffmann, V., Kotlia, B.S., 2003. Palaeoclimatic significance of magnetic properties from the Late Quaternary lacustrine sediments at Pithoragarh, Kumaun Lesser Himalaya, India. Quat. Int. 108, 51–62.
Phartiyal, B., Srivastava, P., Sharma, A., 2009. Tectono-climatic signatures during late Quaternary period from Spiti valley, NW Himalaya, India. Himal. Geol. 30 (2), 164–174.
Phartiyal, B., Singh, R., Kothyari, G Ch, 2015. Late-Quaternary geomorphic scenario due to changing depositional regimes in the Tangtse Valley, Trans-Himalaya, NW India. Palaeogeogr. Palaeoclimatol. Palaeoecol. 422, 11–24.
Phartiyal, B., Sharma, A., Kothyari, G.C., 2013. Damming of river Indus during Late Quaternary in Ladakh region of Trans-Himalaya, NW India: Implications to Lake formation-climate and tectonics. Chin. Sci. Bull. 58, 142–155.
Rawat, S., Gupta, A.K., Sangode, S.J., Srivastava, P., Nainwal, H.C., 2015. Late Pleistocene-Holocene vegetation and Indian summer monsoon record from the Lahaul, northwest Himalaya, India. Quat. Sci. Rev. 114, 167–181.
Richards, B.W.M., Benn, D.I., Owen, L.A., Rhodes, E.J., Spencer, J.Q., 2001. Timing of late Quaternary glaciations south of Mount Everest in the Khumbu Himal, Nepal. Geol. Soc. Am. Bull. 112, 1621–1632.
Robinson, S.G., 1986. The Late Pleistocene paleoclimatic record of North Atlantic deep-sea sediments revealed by mineral magnetic measurements. Phys. Earth Planet. Int. 42, 22–47.
Schmidt, A.M., Von Dobeneck, T., Bleil, U., 1999. Magnetic characterization of Holocene sedimentation in the south Atlantic. Palaeoceanography 14, 465–481.
Schulz, H., von Rad, U., Erlenkeuser, H., 1998. Correlation between Arabian Sea and Greenland climate oscillations of the past 110,000 years. Nature 393 (6680), 54–57.
Searle, M.P., Godin, L., 2003. The South Tibetan Detachment and the Manaslu Leucogranite: a structural Reinterpretation and Restoration of the Annapurna-Manaslu Himalaya, Nepal. Geology 111 (5), 505–523.
Selvaraj, K., Chen, C.T.A., 2006. Moderate chemical weathering of subtropical Taiwan: constraints from solid-phase geochemistry of sediments and sedimentary rocks. J. Geol. 114, 101–116.
Sharma, K.K., Gu, Z.Y., Lal, D., Caffee, M.W., Southon, J., 1998. Late Quaternary morphotectonic evolution of Upper Spiti Valley: a cosmogenic radionuclide study of river polished surfaces. Curr. Sci. 75 (4), 366–372.
Sharma, S., Chand, P., Bisht, P., Shukla, A.D., Bartarya, S.K., Sundriyal, Y.P., Juyal, N., 2016. Factors responsible for driving the glaciation in the Sarchu Plain, eastern Zanskar Himalaya, during the late Quaternary. J. Quat. Sci. 31 (5), 495–511.
Sinha, A., Cannariato, K.G., Stott, L.D., Li, H.-C., You, C.-F., Cheng, H., Edwards, R.L., Singh, I.B., 2005. Variability of southwest Indian summer monsoon precipitation during the Bolling-Allerod. Geology 33, 813–816. http://dx.doi.org/10.1130/G21498.1.
Singh, G., Agrawal, D.P., 1976. Radiocarbon evidence for deglaciation in northwestern Himalaya, India. Nature 260, 233.
Taylor, P.J., Mitchell, A.W., 2000. The Quaternary glacial history of the Zanskar range, north-west Indian Himalaya. Quat. Int. 65, 81–99.
Thompson, R., Oldfield, F., 1986. Environmental Magnetism. Allen and Unwin Publishers Ltd, UK, p. 227.
Valdiya, K.S., Kotlia, B.S., 2001. Fluvial geomorphic evidence for Late Quaternary reactivation of a synclinally folded nappe in Kumaun Lesser Himalaya. J. Geol. Soc. India 58 (4), 303–317.
Van Campo, E., Gasse, F., 1993. Pollen and diatom-inferred climatic and hydrological changes in Sumxi Co Basin (Western Tibet) since 13,000 yr B.P. Quat. Res. 39, 300–313.
Van Campo, E., Cour, P., Sixuan, Hang, 1996. Holocene environmental changes in Bangong Co basin (Western Tibet), Part 2: the pollen record. Palaeogeogr. Palaeoclimatol. Palaeoecol. 120, 49–63.
Wang, Y.J., Cheng, H., Edwards, R.L., An, Z.S., Wu, J.Y., Shen, C.C., Dorale, J.A., 2001. A high-resolution absolute-dated late Pleistocene monsoon record from Hulu Cave, China. Science 294, 2345–2348.
Walden, J., Smith, J.P., Dackombe, R.V., Rose, J., 1995. Mineral magnetic analyses of glacial diamicts from the midland valley of Scotland. Scott. J. Geol. 31, 79–89.
Wheeler, A.J., Oldfield, F., Orford, J.D., 1999. Sedimentology and postdepositional controls on magnetic signals from salmarshes on the north-west coast of Ireland. Sedimentology 46, 545–558.
White, K., Walden, J., Drake, N., Eckardt, F., Settle, J., 1997. Mapping the iron oxide content of dune sands, Namib Sand Sea, Namibia, using Landsat thematic mapper data. Remote Sens. Environ. 62, 30–49.
Wünnemann, B., Demske, D., Tarasov, P., Kotlia, B.S., Reinhardt, C., Bloemendal, J., Diekmann, B., Hartmann, K., Krois, J., Riedel, F., Arya, N., 2010. Hydrological evolution during the last 15 kyr in the Tso Kar lake basin (Ladakh, India), derived from geomorphological, sedimentological and palynological records. Quat. Sci. Rev. 29 (9), 1138–1155.
Wünnemann, B., Reinhardt, C., Kotlia, B.S., Riedel, F., 2008. Observations on the relationship between lake formation and permafrost activity during the last 20,000 years in the Tsokar basin, Ladakh, India. Permafr. Periglac. Process. 19 (4), 341–358.
Yan, G., Wang, F.B., Shi, G.R., Li, S.F., 1999. Palynological and stable isotopic study of palaeoenvironmental changes on the northeastern Tibetan plateau in the last 30,000 years. Palaeogeogr. Palaeoclimatol. Palaeoecol. 153, 147–159.
Yu, L., Oldfield, F., 1989. A multivariate mixing model for identifying sediment source from magnetic measurements. Quat. Res. 32, 168–181.
Yuan, D., Cheng, H., Edwards, R.L., Dykoski, C.A., Kelly, M.J., Zhang, M., Qing, J., Lin, Y., Wang, Y., Wu, J., Dorale, J.A., An, Z., Cai, Y., 2004. Timing, duration, and transitions of the last interglacial Asian monsoon. Science 304, 575–578. http://dx.doi.org/10.1126/science.1091220.
Zhao, Y., Yu, Z., Chen, F., Ito, E., Zhao, C., 2007. Holocene vegetation and climate history at Hurleg Lake in the Qaidam Basin, northwest China. Rev. Palaeobot. Palynol. 145 (3–4), 275–288.
Zhang, C., Mischke, S., 2009. A Lateglacial and Holocene lake record from the Nianbaoyeze Mountains and inferences of lake, glacier and climate evolution on the eastern Tibetan Plateau. Quat. Sci. Rev. 28, 1970–1983.
Zhu, Q., Jinhai, H., Wang, P., 1986. A study of circulation differences between East Asian and Indian summer monsoons with their interaction. Adv. Atmos. Sci. 3 (4), 466–477.